Environmental Science Processes & Impacts

ROYAL SOCIETY OF CHEMISTRY

PAPER

View Article Online
View Journal | View Issue

Cite this: *Environ. Sci.: Processes Impacts*, 2024, **26**, 2010

Physicochemical properties and their impact on ice nucleation efficiency of respiratory viral RNA and proteins†

Mattie Hibbs, [a] Devendra Pal, [a] Gorjana Barudzija[b] and Parisa A. Ariya *[ab]

Ice nucleation processes in the earth's atmosphere are critical for cloud formation, radiation, precipitation, and climate change. We investigated the physicochemical properties and ice nucleation potential of selected viral aerosols, including their RNA and proteins, using advanced techniques such as scanning-transmission electron microscopy (S/TEM), small angle X-ray scattering (SAXS), particle analyzers, and a peltier chamber. The experiments revealed that RNA particles obtained from MS2 bacteriophage had a mean freezing point of −13.9 ± 0.3 °C, comparable to the average ice nucleation temperature of global dust particles, which is approximatively −15 °C. RNA from MS2, Influenza, SARS-CoV-1 and SARS-CoV-2 demonstrated average ice nucleation temperatures of −13.9 ± 0.3 °C, −13.7 ± 0.3 °C, −13.7 ± 0.3 °C, and −15.9 ± 0.4 °C, respectively. SAXS analysis indicated a high local crystallinity value of 0.5 of MS2 RNA particles, hinting that high crystalline nature may contribute to their effectiveness as ice nuclei. Dilution experiments show that viral RNA consistently catalyzes ice nucleation. The addition of dust-containing particles, such as Fe_2O_3, CuO, and TiO_2, to MS2 bacteriophage droplets enhanced ice nucleation, as did UV radiation. We herein discuss the implications of this work on ice nucleation and freezing processes.

Received 8th July 2024
Accepted 25th September 2024

DOI: 10.1039/d4em00411f

rsc.li/espi

Environmental significance

Ice nucleation plays a critical role in cloud formation, thus impacting the global radiation budget. Examining the physicochemical properties of ice nucleating particles is essential to improve our understanding of ice nucleation processes. Numerous studies have characterized the ice nucleation properties of bio-aerosols, including bacteria, fungi, and pollen, but there is only one study to our knowledge which examines the ice nucleation potential of viruses. Our study is the first to show that selected respiratory viruses including SARS-CoV-2 can serve as efficient ice nuclei. Surface property analysis, namely small-angle X-ray scattering, revealed that crystallinity and polydispersity are potential drivers of ice nucleation abilities. This work contributes to the fundamental research in understanding bioaerosols and climate interactions.

Introduction

The Intergovernmental Panel on Climate Change (IPCC)[1,2] has identified airborne particles, or aerosols, as a priority research area for air quality and climate change. Air pollution and, notably, small aerosols cause around 7 million premature deaths every year globally, making them an important topic in health science research.[3] Furthermore, aerosols are critical in several atmospheric processes, including cloud formation, precipitation, the radiation budget, and global climate change.[4] Understanding the physicochemical properties such as size, shape, abundance, and surface topography of aerosols, particularly bioaerosols, is crucial for assessing their role in aerosol–cloud interactions.[5–7]

Bioaerosols are aerosols of biological origin or those containing biological parts or derivatives, including bacteria and viruses.[8] Viruses exist ubiquitously in the natural environment, including in soil, water, and air. Their numbers are greater than any other biological entity with an estimated 10 nonillion (10^{31}) individual viruses on Earth.[9,10] Airborne viruses can interact with other aerosol particles in the atmosphere and may undergo physicochemical transformations and long-range transportation.[11] These physicochemical changes are influenced by the aerosols' microphysical characteristics and by atmospheric conditions such as humidity, temperature, and radiation.[12–15] Although a comprehensive understanding of the physicochemical properties of bioaerosols is necessary for assessing their impact on atmospheric chemistry processes and epidemiological processes (uptake and transport mechanisms),[16,17]

[a]*Department of Atmospheric and Oceanic Sciences, Canada. E-mail: parisa.ariya@mcgill.ca*

[b]*Department of Chemistry McGill University, 801 Sherbrooke St. W., Montreal, QC, H2A 0B8, Canada*

† Electronic supplementary information (ESI) available. See DOI: https://doi.org/10.1039/d4em00411f

their role as ice and cloud condensation nuclei remain active research areas.

In recent decades, various emerging contaminants have been identified as effective ice nuclei, specifically contaminants originating from nano/microplastics,[18] metal–organic complexes,[19] and pharmaceutical materials.[20] Dust particles are known to be the most abundant type of ice nucleating particles in the atmosphere, while certain bioaerosols are among the most efficient.[21,22] For example, *Pseudomonas syringae* bacteria have evolved to induce ice nucleation within a temperature range of approximately −2 to −7 °C.[23] In comparison, dust particles exhibit ice nucleation abilities around −15 °C.[21,24] The ice nucleation mechanisms of various bioaerosols including pollen,[25] fungi,[26] and bacteria[23] have been extensively studied, but very little is known about the ice nucleation ability of airborne viruses.[27]

In this study, we investigated the ice nucleation abilities of airborne viruses and their RNA, along with the impact of mixing the viruses with dust particles. We conducted microphysical experiments focusing on MS2 Bacteriophage (also termed Bacteriophage MS2 or MS2), a single-stranded RNA virus which infects *Escherichia coli*. MS2 is a commonly found virus and, along with other bacteriophages, serves as a good surrogate for studying airborne viruses.[28] Additionally, we assess the ice nucleation abilities of selected virus particles, such as SARS-CoV-1 RNA, SARS-CoV-2 RNA and proteins, RNA from human influenza, and heat-inactivated SARS-CoV-2 (COVID-19). Furthermore, we investigated the surface properties of viruses to understand their potential role in ice nucleation mechanisms.

Methods

Ice nucleation – immersion-mode drop freezing experiments

A common way to study the ice nucleating ability of ice nucleating particles (INPs) is drop freezing assay experiments, which have been shown by Vali[29] to be an accurate method for calculating the active ice nuclei content of the solution from which the droplets were formed. Drop freezing experiments are characterized by the simultaneous cooling of equal-sized droplets until frozen, and the freezing point of each droplet is recorded. Based on the observed freezing temperatures, the differential nuclei concentration $k(T)$ can be obtained (Methods: Ice nucleation – analysis, eqn (1)).

In this study, we conducted drop freezing assays of viral droplets using a laboratory-built ice nucleation apparatus.[30,31] In brief, solutions containing either viral particles or some mixture of viral particles with other common aerosols, were made by dilution using ultrapure Milli-Q water (18.2 MΩ cm Milli-Q Synergy UV system, Millipore Sigma, USA). MS2 viral solutions were prepared at varying concentrations of 100×, 200× and 330× and all additional particles were present in solutions at a 0.1% by mass concentration. To ensure an even distribution of particles, all solutions were vortexed. Each experiment was comprised of approximately 120 droplets of equal volume (10 μL, with radius of approximately 1.34 μm) deposited onto a vaseline-coated copper plate and replicated trice. Once each droplet was placed uniformly on the freezing plate, the plate was cooled at a constant rate of 0.9 degrees centigrade per minute, and the temperature at which the liquid droplet solidified was recorded. To verify that all freezing events were captured, we recorded a video for cross-verification.

We also investigated the impact of mixing with dust particles (nanosized TiO_2, Fe_2O_3 and CuO) and UV exposure on the ice nucleation ability of MS2. To examine how ice nucleation changes when viral droplets are clustered together, designated samples were briefly centrifuged for about 2–5 minutes to promote particle agglomeration. To assess the impact of light on viral droplets, MS2 samples are exposed to UVA (315–400 nm) or UVB (280–315 nm) irradiation for 30 minutes.

Ice nucleation – analysis

The differential nuclei concentration $k(T)$ (in L^{-1}) describes the average number of ice nuclei in a temperature interval, $n(T)$, per unit of volume, V, and can be expressed as:

$$k(T) = \frac{n(T)}{V}, \quad (1)$$

Upon algebraic rearrangement and integration, the cumulative concentration of active ice nuclei, $K(T)$ (in L^{-1}) is obtained:

$$K(T) = \frac{\ln N_0 - \ln N(T)}{V}, \quad (2)$$

where N_0 is the number of droplets in the initial population and $N(T)$ is the number of unfrozen droplets at temperature T.[29]

All data processing, statistical analysis methods, and plotting methods/software are discussed in Methods: Statistical analysis and plots.

Litesizer particles sizer

Litesizer particle sizer 500 (PSA, Anton Paar) was used to analyze the particle diameters of MS2 samples. The PSA instrument uses dynamic light scattering to obtain information about the physical properties of the samples. Three measurements were made for each sample at 25C with the default measurement angles of 15°, 90°, and 175°. This analysis yielded the diffusion coefficients and transmittances.

Electron microscopy imaging

Talos F200X scanning/transmission electron microscope (S/TEM) was used. Talos combines high resolution S/TEM and TEM imaging, with energy dispersive X-ray spectroscopy (EDS), which allows signal detection and elemental analysis of selected areas. The imaging was performed by Facility for Electron Microscopy Research at McGill University. Bacteriophage MS2 was prepared for S/TEM imaging by staining with uranyl acetate and the Spirit 120 kV TEM is used for imaging. Another set of MS2 samples was prepared without uranyl acetate staining to determine the composition of the material on the grid and imaged in the Talos F200X 200 kV TEM.

Heat inactivation of SARS-CoV-2 viruses

In a biosafety 3 laboratory, a specific volume of SARS-CoV-2 was heat-inactivated at 92 °C for 1 hour with continuous shaking to ensure biosafety during subsequent handling in a biosafety level 1 laboratory setting. BLAST results of sequenced genome confirmed SARS-CoV-2 identity (Fig. S2†). Fig. S1† shows the heat inactivation images of SARS-CoV-2 viral load sample, and genomic data are provided in the ESI (Fig. S1 and S2†). Methods for heat inactivation of SARS-CoV-2 usually use temperatures of around 56–60 °C (ref. 32–34) although those methods are typically used to only reduce the viral activity when the sample is needed for serological assays. A few studies have also examined the remaining infectivity when SARS-CoV-2 samples are exposed to 80 °C for 1 hour,[35] 92 °C for 15 minutes[34] and 95 °C for 3 minutes.[35] We performed heat inactivation at 92 °C for 20 minutes; viral activity is still observed and therefore the exposure time is increased to one hour.

To confirm no remaining live virus, the inactivated virus was tested by inoculating host cells. The test sample is passaged twice; the first passage is incubated for 3 days, and the second passage is incubated for 7 days. Vero E6 confluent monolayers were infected with SARS-CoV-2 virus (MOI 0.05), heat-inactivated SARS-CoV-2, and monitored for cytopathic effect (CPE). On day 3, the supernatant was removed, spun down to remove any cell debris, and then transferred to a new lot of Vero E6 confluent monolayers and monitored for 7 days. Heat-Inactivated SARS-CoV-2 using this protocol did not cause infection as determined by the lack of CPE in the inoculated Vero E6 cells. RIM-1, lineage B.1.147 was used for heat-killed samples (formally called CP13.32) which is SARS-CoV-2 that is propagated from a McGill University Health Center (MUHC) patient sample from March/April 2020. The RIM-1 viral stocks were whole genome sequenced, and the GenBank accession number is MW599736. Images of inactivated viruses are given in ESI Fig. S1.†

Small angle X-ray scattering (SAXS) analysis

The SAXSpoint 2.0 (Anton Paar, Austria) at McGill University was used to analysis physical properties of MS2 bacteriophage samples. The SAXS instrument employed CuKα radiation source with a wavelength (λ = 1.54 Å) and an Eiger R 1M (Horizontal) detector. The source-to-detector distance was set at 576.33 mm for the experiments. 30 μL of sample volume was used during each experiment and placed in quartz capillary (1 mm, Anton Paar). During each measurement, a total of 3 frames were recorded with 20 minutes per frame of X-ray exposure. The obtained SAXS profiles were corrected as a function of the scattering vector ($q = (4\pi/\lambda)\sin\theta$, where 2θ is the scattering angle). Data analysis of the SAXS measurements is performed using SasView 5.0.4 software, an open-source code widely used for SAXS data analysis.[36] The Milli-Q water was used as background data; it has been subtracted from all the measured samples and the normalized dataset was used for subsequent analysis (SAXSpoint2). The SasView software is also used for Guinier analysis to check the data quality. Correlation function analysis was performed to extract the surface properties, including the polydispersity, average core thickness, and local crystallinity of each sample. The user specified the q-ranges of analysis, and the software extracted these properties/parameters using a Guinier function to fit the designated low-q range values, and a Porod model for fitting the high-q range values.[37]

Polydispersity is calculated in the software by dividing the standard deviation of the size distribution by the mean size value. Local crystallinity is calculated by dividing the average hard block thickness (L_c) by the long period (L_p).

Statistical analysis and plots

Various statistical analyses were performed to investigate the ice nucleation efficiency of the different samples. The reported results include 1st and 99th percentiles, along with median and average values. Two-sample t-tests were performed in RStudio using the t-test function, in which it assumed that the two populations have different variances. Standard errors were calculated *via* the following equation appropriate for large sampling data, where σ corresponds to the standard deviation and N is the sample size.

$$\mathrm{SE} = \sigma \Big/ \sqrt{N} \tag{3}$$

All graphs were made in RStudio. Data is publicly available on the Borealis data repository.[38]

Materials and supplies

The metal oxides used were TiO_2, Fe_2O_3, and CuO; they were purchased from Sigma-Aldrich in nanoparticle form. SARS-CoV-1 RNA and RNA from Bacteriophage MS2 (product code: 10 165 948 001) were purchased from Sigma-Aldrich. Bacteriophage MS2 (0 810 052) was manufactured by Zeptometrix Corporation and supplied by Cedarlane Laboratories. Influenza RNA (VR-95DQ) was manufactured by American Type Culture Collection and supplied by Cedarlane Laboratories. SARS-CoV-2 RNA (ssRNA) (EURM019) was supplied by the Joint Research Centre (European Commission), and proteins were supplied by Life Technologies Inc. SARS-CoV-2 was propagated and then heat inactivated in a BSL3 laboratory at the Research Institute of the McGill University Health Centre (RI MUHC).

A note on terminology

In this paper, we use the terms virus and viral particle. Virus is the general term for what we are studying; SARS-CoV-1, SARS-CoV-2, influenza, and MS2 bacteriophage are all viruses. A viral particle is a particle containing viral material.

Results and discussions

In this study, we conduct a comprehensive series of ice nucleation microphysics experiments involving various viral components, including the model virus MS2 Bacteriophage and its RNA, heat-inactivated SARS-CoV-2 (COVID-19), SARS-CoV-2 RNA, and SARS-CoV-1 RNA and proteins. Our goal was to

investigate the effectiveness of the ice nucleation abilities of these viral components and compare the results with proxy dust particles. Furthermore, we explored the influence of mixing with dust particles and the impact of UV radiation on the virus' respective ice nucleation abilities. A summary of the mean freezing ice nucleation temperatures of various samples is given in Fig. 1.

Ice nucleation of bacteriophage MS2: impact of UV light exposure

Fig. 1 and 2a show the mean freezing temperatures from drop-freezing experiments for MS2 Bacteriophage at different dilutions (100×, 200×, 330×). The mean freezing temperatures for samples of MS2 Bacteriophage at 100×, 200× and 330× dilutions were −16.5 ± 0.3, −18.8 ± 0.3, and −18.2 °C, respectively (Fig. 1, red box; Table 1). We observed that the mean freezing temperatures decreased by about 2 °C with an increased dilution factor from 100× to 200×, and no significant change in subsequent dilutions. This may likely be due to decreased particle concentration affecting ice nucleation site availability, thus slowing down the catalytic process.[39] Interestingly, MS2 RNA exhibited a mean freezing temperature of −13.9 ± 0.3 °C, indicating RNA's potential role in ice nucleation (Fig. 1).

To investigate the impact of irradiation on the ice nucleation ability of airborne viruses, we exposed 100× diluted MS2 samples to UVA (315–400 nm) and UVB (280–315 nm). The mean freezing values of UVA- and UVB-exposed MS2 samples were −13.4 ± 0.4 and −12.6 ± 0.3 °C, respectively (Table 1), and the cumulative nucleus concentration of photolyzed MS2 and centrifuged photolyzed MS2 samples are shown in Fig. 2b. A *t*-test ($p = 0.108$) confirmed no significant difference in ice nucleation results between UVA-*versus* UVB-exposed MS2-100× samples, but a significant ($p \ll 0.00001$) difference was indeed observed between untreated MS2-100× mean freezing temperatures and both UV-treated samples (Fig. 1 and 2b). As shown in Table 1, UVA exposure elevated the freezing temperature by −3.1 °C and UVB elevated it by −3.9 °C. This indicates that UV radiation may increase the ice nucleation potential.

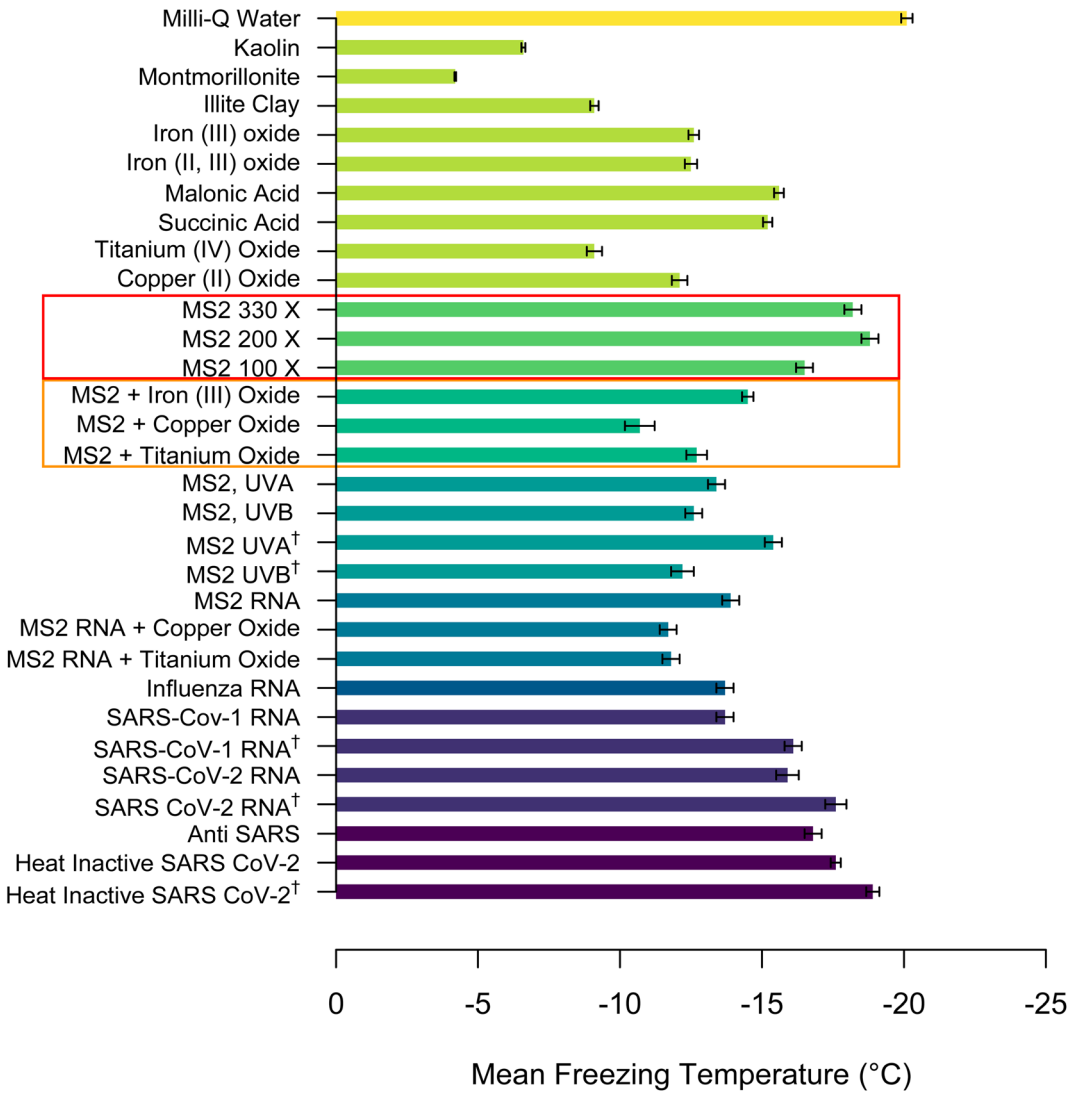

Fig. 1 Mean freezing temperatures from drop freezing experiments of various samples; †centrifuged.

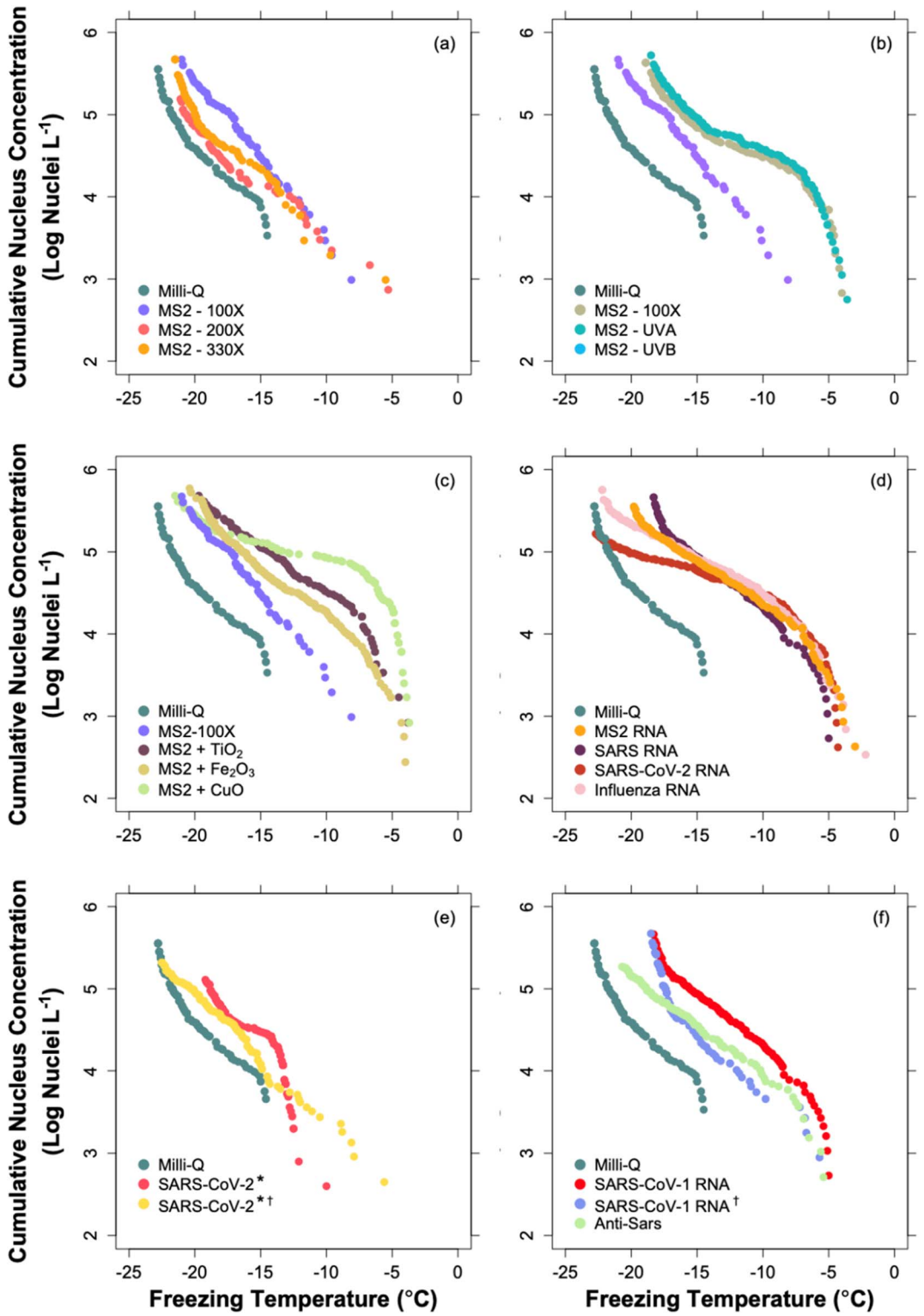

Fig. 2 Comparison of the cumulative nucleus spectra obtained from drop-freezing experiments of different samples and their respective treatments. (a) MS2 at dilutions 100×, 200×, and 330×; (b) UVA- and UVB-treated MS2 samples; (c) MS2 solutions mixed with TiO_2, Fe_2O_3, and CuO; (d) untreated viral RNA from: MS2, SARS-CoV-1 (SARS), SARS-CoV-2, and human influenza (e) SARS-CoV-2 treatments: heat-inactivated (*) and centrifuged (†); (f) SARS-CoV-1 RNA: untreated and centrifuged (†).

Mixing MS2 with dust-like particles: impacts on ice nucleation

We examined the impact of mixing MS2 with common metal oxides found in dust particles such as TiO_2, Fe_2O_3 and CuO nanoparticles. We exposed viral MS2-100× dilution samples at 0.1% solutions of TiO_2, Fe_2O_3, and of CuO. The mean freezing temperatures are given in Fig. 1 (orange box) and Fig. 2c shows

Table 1 Freezing temperature summary statistics from drop-freezing experiments involving different preparations of MS2 samples, including various dilution factors and UV treatments

Statistic (°C)	Mean	Median	1st percentile	99th percentile	Standard error ($\sigma/\sqrt{N}$)
Reference/blank					
Milli-Q water	−20.5	−21.3	−22.9	−16.8	0.2
MS2 dilutions					
MS2 100×	−16.5	−16.9	−20.1	−9.6	0.3
MS2 200×	−18.8	−19.8	−21.6	−7.7	0.3
MS2 330×	−18.2	−19.5	−21.5	−9.8	0.3
MS2 100×, UV treatments					
MS2 100×	−16.5	−16.9	−20.1	−9.6	0.3
MS2 100×, UVA	−13.3	−14.9	−19.1	−4.3	0.4
MS2 100×, UVB	−12.6	−14.3	−18.5	−4.2	0.3

the cumulative nucleus concentration of MS2 compared with the mixtures of MS2 with dust particles. The mean freezing temperatures of MS2-100× diluted sample alone was −16.5 ± 0.3 °C; when MS2 was mixed with TiO_2, Fe_2O_3 and CuO, the freezing temperatures increased to −12.7 ± 0.2 °C, −14.4 ± 0.2 and −10.7 ± 0.3 °C, respectively. These findings suggest that the presence of dust particles can enhance the ice nucleation ability of viral particles, likely due to increased surface area and effective ice nucleation sites provided by the dust particles.[40] A statistically significant difference ($p < 0.05$) is found between the mean freezing temperatures MS2-100× sample, and the MS2-100× mixture samples. Fig. S3 and S4 in ESI† show the cumulative nucleus concentrations of a selection of airborne particles (Fig. S3†) as well as TiO_2, Fe_2O_3, and CuO (Fig. S4†).

Ice nucleation of SARS-CoV-2, RNA and related samples

Heat inactive SARS-CoV-2 had a mean freezing temperature of −17.6 ± 0.4 °C, which decreased further upon centrifugation to −18.9 ± 0.2 °C. It is essential to consider that the heat inactivation process may lead to the presence of fragmented RNA and protein shells in the sample, potentially affecting its ice nucleation behavior. Ice nucleation of these coronaviruses-related samples show that even when a viral droplet contains an inactive virion, it still has the potential to be a good INP.

Furthermore, we investigated the ice nucleation efficiency of several RNA samples considering many airborne viruses are RNA viruses.[41] The ice nucleation efficiencies of RNA from MS2, SARS-CoV-1, SARS-CoV-2, and Influenza was investigated. Viral RNA, enclosed within the capsid, can degrade under certain atmospheric conditions, such as high relative humidity or reactive oxygen species (ROS), potentially leaving RNA fragments in the atmosphere.[42] Viral RNA exhibits high mutation rates and morphological diversity,[43] making it suitable for studying ice nucleation processes that depend on particle structure and morphology.[40]

The ice nucleation efficacy and cumulative nucleus concentrations of RNA from MS2, SARS-CoV-1, SARS-CoV-2, are shown in Fig. 2d. The mean freezing temperatures of RNA from MS2, SARS-CoV-1, and Influenza were −13.9 ± 0.3 °C, −13.7 ± 0.3 °C, and −13.7 ± 0.3 °C, respectively (Fig. 1), revealing that RNA freezes at warmer temperature than some ice-nucleating dust particles (Fig. 1). Fig. 2e and f show the cumulative nucleus concentrations of SARS-CoV-1 RNA and SARS-CoV-2 RNA as well as the centrifuged samples. Centrifugation in these experiments did not significantly affect the ice nucleation abilities of either RNA type.

In this study, our primary focus has been on using deactivated viruses to ensure health and safety during the experiments in our microphysics labs, acknowledging that the ice nucleation behavior is expected to be altered. Furthermore, some S/TEM and BET facilities cannot host even deactivated viruses. Using different preparation methods, all RNA tested display ice nucleation efficiency, demonstrating that the various methods of RNA isolation are not likely the cause of ice nucleation, but that the RNA itself is. It is important to clarify that when we refer to RNA as an ice-nucleating particle, we are considering the entire structure of the RNA, including the capsomeres. However, we do not make specific claims about whether the ice nucleation ability resides strictly in the genetic material or within the capsid's system, as that is beyond the scope of this paper. Yet, we recommend future research in this domain.

Surface properties and ice nucleation efficiency

Small-angle X-ray scattering (SAXS) measurements provide crucial insight into the nanoscale density differences in both solid and aqueous samples.[44,45] These density differences determine the particles size distribution, shape, dispersity (monodispersed and polydispersity) pore size, and local crystallinity, which are essential for assessing ice nucleation capabilities.[17,46] The scattering data obtained from SAXS measurement contains information on the size, shape, orientation, squared contrast, weighted concentration, and volume of the particles.[37] For this study, we used SasView 5.2 software for correlation function analysis to estimate the changes in phase or orientation change in particles, affecting local crystallinity (phase) of the materials.[36] Table 2 presents the local crystallinity and polydispersity of MS2 samples. Polydispersity measures the width of the size distribution of correlation function decay rates and not the particle size distribution.[47] The change in phase (local crystallinity) and polydispersity of

Table 2 Physical properties of MS2 samples extracted from SAXS data with SasView software. Properties include polydispersity, average core thickness, and local crystallinity. Diffusion coefficients and transmittances from two of three trials for each MS2 sample, obtained from the Litesizer 500 particle sizer (Anton Paar) are also given

SAXS correlation function analysis parameters

Sample	Polydispersity	Avg. core thickness (Å)	Local crystallinity
MS2 100×	2.44	9.2	0.51
MS2 200×	2.40	7.0	0.39
MS2 330×	2.79	7.2	0.28

Litesizer particle sizer physical properties

	Diffusion coefficient ($\mu m\ s^{-1}$)		Transmittance	
Sample	Measurement 1	Measurement 2	Measurement 1	Measurement 2
Mill-Q water	0.74	0.62	87.5%	87.6%
MS2 100×	1.60	1.83	87.2%	87.2%
MS2 200×	1.82	1.48	87.9%	87.9%
MS2 330×	1.59	1.59	87.7%	87.7%
Fe_2O_3 + MS2 + Milli-Q	4.68	4.76	10.6%	10.9%

material significantly impacts the ice nucleation capability of materials.[20,37]

In this study, we analyzed three MS2 samples (100×, 200× and 330×) to understand their physical properties and their role in ice nucleation mechanism. The MS2 100× sample exhibited higher local crystallinity and similar polydispersity compared to MS2 200× and MS2 330×, shown in Table 2. The combination of high polydispersity and local crystallinity likely makes the MS2 100× sample more efficient at ice nucleation (Table 1). A higher degree of crystallinity suggests a greater potential for the sample to organize neighboring water molecules into ice-like crystal formations, enhancing its ice nucleation capability.[20,40] Conversely, MS2 330×, with slightly higher polydispersity but significantly lower local crystallinity, and MS2 200×, with similar polydispersity but lower crystallinity than MS2 100×, show ice nucleation at cooler temperatures (Fig. 1). Therefore, a higher degree of crystallinity suggests a stronger ice nucleation capability.

The overall effectiveness of ice nucleation depends on the combined effect of both local crystallinity and polydispersity. Previous studies have shown that materials with high crystallinity and polydispersity often have polymorphic surfaces that lower the free energy, facilitate local structuring upon cooling, and promote crystallization in a supercooled state.[20,37,47,48] For example, efficient atmospheric ice nuclei, such as silver iodide and *Pseudomonas syringae* bacteria, nucleate ice at relatively warmer temperatures due to their crystallinity, symmetry, and size, which allow them to adopt structures closer to hexagonal ice at supercooled temperatures.[37,49] Density, poly-surfaces, and polydispersity are control parameters that induce crystallization and favor structures acting as precursors for the ice nucleation process.

The SAXS intensity counts of the three different MS2 dilution samples are shown in Fig. 3. The observations suggest the MS2-100× had the highest scattering intensity, while the more diluted samples had very similar scattering patterns to each other. These results are likely due to the increased concentration of viral particles in the 100× solution. Further dilutions have reduced viral particles concentrations, and thus they more closely freezed/resemble the Milli-Q blank (Table 1).

Furthermore, Litesizer particle sizer data includes the diffusion coefficients and transmittance, shedding light on surface physiochemistry (Table 2). These coefficients provide valuable information about the movement of particles, dispersion, and stability in the solution and the extent to which light is transmitted through the sample. These are not necessarily predictors of excellent or poor ice nuclei but serve as supplemental data to show the internal structure of a solution of viral particles in water. We see no significant difference between water and viral solutions' transmittance and diffusion properties but a considerable difference between these samples and the mixtures with dust particles.

Can airborne viruses be important in ice nucleation?

Aerosols are seeds for cloud formation,[4] and as stated, one of the significant uncertainties in climate change predictions.[50] During the last decades of bioaerosol research on ice nucleation, it has become evident that bioaerosols and their remnants can act as efficient ice nuclei.[21,22] There are several studies which have quantified the microbial concentrations in the planetary boundary layer[51,52] and at higher altitudes relevant to cloud formation.[53–55] However, despite the known abundance

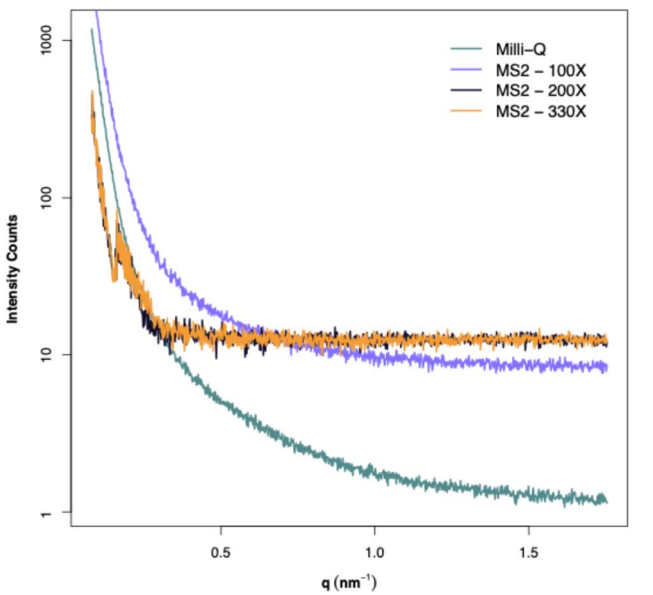

Fig. 3 Intensity counts of MS2 at 100×, 200× and 330× dilutions obtained from SAXS analysis plotted on a log-scale.

of viruses compared to bacteria in ambient air, there are no studies to our knowledge which specifically investigate their role in cloud formation. Further work should be done to assess the concentrations of viruses at cloud-relevant heights.

The amount of airborne virus at a given time varies due to several factors, namely droplet size, evaporation rate, gravitational settling, and the viral load.[56,57] These factors make calculating airborne viral concentrations complex and subject to many limitations. Additionally, there is an abundance of environmental conditions which can affect the interaction of airborne viruses with other aerosols and their behaviour in the context of ice nucleation. These environmental factors include humidity, radiation (particularly UVC) and temperature.[58–60] Once the virus enters the air, it is subject to all of these environmental factors and interactions with other particles. Notably, viruses are smaller in size than bacteria and course dust particles, and thus may have longer residence times and experience similar or even longer ranges of transport.[61,62] Even if the virus is not active or completely intact, this work has shown that select viruses may still retain their ice nucleation abilities. Such microphysical processes they may undergo at this stage are understudied and deserve further research is required.

Current research has shown that some airborne viruses including MS2 bacteriophage, SARS-CoV-1 and SARS-COV-2 and their remanent RNA have distinct physicochemical surfaces properties that allow them to act as effective ice nuclei at temperatures comparable to those of dust particles, which have long been considered one of the most critical global ice nuclei in the Earth's atmosphere.[21,41] Like dust particles, viruses are present in massive quantities, experience transport through air, and some have been shown to effectively facilitate ice nucleation at temperatures between −13 and −17 °C. The earlier work done by Adams *et al.* (2021)[27] suggests that they may play a more important role in the composition of marine environment INPs than those of terrestrial environments. Yet, there are many unknowns. Hereby, we recommend further observation, laboratory, and modelling experiments to accurately evaluate their importance.

Concluding remarks

In this study, we show for the first time that selected RNA of four different respiratory viral entities exhibit mean ice nucleation temperatures up to −13.7 °C. Adding dust-like aerosols to MS2 droplets increases ice nucleation temperatures or makes them more efficient ice nuclei. The combination of high crystallinity and polydispersity in these viruses may partially explain the effectiveness of ice nuclei. The results of this study indicate that some viruses and selected viral structures, such as RNA and proteins, might have the ability to be effective ice nuclei.

Ice nucleation ability in viral structures opens new avenues for understanding water uptake in viral processes, which may have significant implications for the transmission of respiratory viruses indoors and outdoors. As we learned from decades of bioaerosol nucleation research,[6,63,64] airborne pathogenic particles, including some viruses and bacteria, exhibit an extensive range of ice nucleation abilities that should be explored. As viral entities such as viral RNA and proteins are ubiquitous in natural surface waters, it is crucial to delve deeper into the impact of viruses on freezing processes in these environments. With technological advances, including ice nucleation, one can better understand many other effective ice nuclei from biological origins or emerging materials from human activities. Our study emphasizes the need for continued research in this domain, with potential implications for atmospheric processes and the frozen water dynamics in natural settings. Understanding the ice nucleation capabilities of viruses could provide valuable insights into climate modelling and the environmental behaviour of airborne pathogens.

Data availability

Data for this article, including.csv files of freezing temperatures and cumulative nucleus concentrations, are available at McGill University Dataverse at **https://doi.org/10.5683/SP3/ZBYBTM**.

Author contributions

Mattie Hibbs: Data curation, formal analysis, investigation, software, visualization, writing – original draft, writing – review and editing. Devendra Pal: investigation, methodology, project administration, software, writing – original draft, writing – review & editing. Gorjana Barudzija: formal analysis, investigation, writing – original draft. Parisa A. Ariya: conceptualization, funding acquisition, methodology, project administration, resources, supervision, writing – original draft, writing – review & editing.

Conflicts of interest

There are no conflicts to declare.

Acknowledgements

This work was supported by the Natural Sciences and Engineering Research Council [NSERC 223464]; the Canadian Foundation for Innovation [CFI 259754]; and PURE NSERC CREATE [251590]. We thank NSERC, NSERC-CREATE PURE, NSERC RTI for financial support. We also acknowledge Dr Vali for electron microscopy, as well as Dr Hatem Titi for SAXS instrument.

References

1 J. E. Penner, M. O. Andreae, H. Annegarn, L. Barrie, J. Feichter, D. Hegg, A. Jayaraman, R. Leaitch, D. Murphy, J. Nganga and G. Pitari, Aerosols, their direct and indirect effects, in *Climate change 2001: the scientific basis*, Contribution of working group I to the third assessment report of the intergovernmental panel on climate change, Cambridge University Press, 2001, pp. 289–348.
2 O. Boucher and D. Randall, *Climate Change 2013 the Physical Science Basis: Working Group I Contribution to the Fifth*

Assessment Report of the Intergovernmental Panel on Climate Change 2013, 2013, pp. 571–658.

3 J. Lelieveld, A. Pozzer, U. Pöschl, M. Fnais, A. Haines and T. Münzel, Loss of life expectancy from air pollution compared to other risk factors: a worldwide perspective, *Cardiovasc. Res.*, 2020, **116**(11), 1910–1917.

4 G. Mhyre, C. L. Myhre, B. H. Samset and T. Storelvmo, Aerosols and their Relation to Global Climate and Climate Sensitivity, *Nature Education Knowledge*, 2013, **4**(5), 7.

5 V. H. Grassian, When Size Really Matters: Size-Dependent Properties and Surface Chemistry of Metal and Metal Oxide Nanoparticles in Gas and Liquid Phase Environments, *J. Phys. Chem. C*, 2008, **112**(47), 18303–18313.

6 P. A. Ariya, J. Sun, N. A. Eltouny, E. D. Hudson, C. T. Hayes and G. Kos, Physical and chemical characterization of bioaerosols – Implications for nucleation processes, *Int. Rev. Phys. Chem.*, 2009, **28**(1), 1–32.

7 R. Rangel-Alvarado, D. Pal and P. Ariya, *$PM_{2.5}$ Decadal Data in Cold vs. Mid-climate Airports: COVID-19 Era and a Call for Sustainable Air Quality Policy*, Rochester, NY, 2021.

8 K.-H. Kim, E. Kabir and S. A. Jahan, Airborne bioaerosols and their impact on human health, *J. Environ. Sci.*, 2018, **67**, 23–35.

9 K. Moelling and F. Broecker, Viruses and Evolution - Viruses First? A Personal Perspective, *Front. Microbiol.*, 2019, **10**, 523.

10 N. S. Clayton and N. J. Emery, What do jays know about other minds and other times?, in *Neurobiology of Umwelt: How Living Beings Perceive the World. Research and Perspectives in Neurosciences*, ed. A. Berthoz and Y. Christen, Springer-Verlag Berlin, Berlin, 2009, pp. 109–123.

11 J. Sun and P. A. Ariya, Atmospheric organic and bio-aerosols as cloud condensation nuclei (CCN): A review, *Atmos. Environ.*, 2006, **40**(5), 795–820.

12 W. Yang and L. C. Marr, Mechanisms by Which Ambient Humidity May Affect Viruses in Aerosols, *Appl. Environ. Microbiol.*, 2012, **78**(19), 6781–6788.

13 V. J. Baboomian, Y. Gu and S. A. Nizkorodov, Photodegradation of Secondary Organic Aerosols by Long-Term Exposure to Solar Actinic Radiation, *ACS Earth Space Chem.*, 2020, **4**(7), 1078–1089.

14 E. Q. Walhout, H. Yu, C. Thrasher, J. M. Shusterman and R. E. O'Brien, Effects of Photolysis on the Chemical and Optical Properties of Secondary Organic Material Over Extended Time Scales, *ACS Earth Space Chem.*, 2019, **3**(7), 1226–1236.

15 American Institute of Aeronautics and Astronautics, The Effects of Temperature and Humidity on Aerosol Optical Properties, *2023 Regional Student Conferences, Region I*, ed. B. Koohbor, J. Ruzskowski, K. Myren, J. Dinse, A. Smith and E. Bering, University at Buffalo, Buffalo, New York, United States of America, 2023.

16 L. Morawska, G. Buonanno, A. Mikszewski and L. Stabile, The physics of respiratory particle generation, fate in the air, and inhalation, *Nat. Rev. Phys.*, 2022, **4**(11), 723–734.

17 D. Pal, M. Amyot, C. Liang and P. A. Ariya, Real-time 4D tracking of airborne virus-laden droplets and aerosols, *Commun. Eng.*, 2023, **2**(1), 1–15.

18 M. Ganguly and P. A. Ariya, Ice Nucleation of Model Nanoplastics and Microplastics: A Novel Synthetic Protocol and the Influence of Particle Capping at Diverse Atmospheric Environments, *ACS Earth Space Chem.*, 2019, **3**(9), 1729–1739.

19 M. Ganguly, S. Dib and P. A. Ariya, Fast, Cost-effective and Energy Efficient Mercury Removal-Recycling Technology, *Sci. Rep.*, 2018, **8**(1), 16255.

20 J. Kaur, M. Ganguly, R. Rangel-Alvardo, D. Pal, R. Hall and P. A. Ariya, Ice Nucleation of Pharmaceutical and Synthetic Organic Emerging Contaminants: The Impact of Selected Environmental Conditions, *ACS Earth Space Chem.*, 2022, **6**(9), 2236–2249.

21 B. J. Murray, D. O'Sullivan, J. D. Atkinson and M. E. Webb, Ice nucleation by particles immersed in supercooled cloud droplets, *Chem. Soc. Rev.*, 2012, **41**(19), 6519–6554.

22 A. Iwata, M. Imura, M. Hama, T. Maki, N. Tsuchiya, R. Kunihisa, *et al.*, Release of Highly Active Ice Nucleating Biological Particles Associated with Rain, *Atmosphere*, 2019, **10**(10), 605.

23 M. Lukas, R. Schwidetzky, R. J. Eufemio, M. Bonn and K. Meister, Toward Understanding Bacterial Ice Nucleation, *J. Phys. Chem. B*, 2022, **126**(9), 1861–1867.

24 C. Hoose and O. Möhler, Heterogeneous ice nucleation on atmospheric aerosols: a review of results from laboratory experiments, *Atmos. Chem. Phys.*, 2012, **12**(20), 9817–9854.

25 S. Hartmann, M. Ling, L. S. Dreyer, A. Zipori, K. Finster, S. Grawe, *et al.*, Structure and Protein-Protein Interactions of Ice Nucleation Proteins Drive Their Activity, *Front. Microbiol.*, 2022, **13**, 872306.

26 S. Pouleur, C. Richard, J.-G. Martin and H. Antoun, Ice Nucleation Activity in Fusarium acuminatum and Fusarium avenaceum, *Appl. Environ. Microbiol.*, 1992, **58**(9), 2960–2964.

27 M. P. Adams, N. S. Atanasova, S. Sofieva, J. Ravantti, A. Heikkinen, Z. Brasseur, D. Jonathan, D. H. Bamford and B. J. Murray, Ice Nucleation by Viruses and Their Potential for Cloud Glaciation, *Biogeosciences Discuss.*, 2021, 1–26.

28 N. Turgeon, M.-J. Toulouse, B. Martel, S. Moineau and C. Duchaine, Comparison of Five Bacteriophages as Models for Viral Aerosol Studies, *Appl. Environ. Microbiol.*, 2014, **80**(14), 4242–4250.

29 G. Vali, Quantitative Evaluation of Experimental Results an the Heterogeneous Freezing Nucleation of Supercooled Liquids, *J. Atmos. Sci.*, 1971, **28**(3), 402–409.

30 R. Mortazavi, C. T. Hayes and P. A. Ariya, Ice nucleation activity of bacteria isolated from snow compared with organic and inorganic substrates, *Environ. Chem.*, 2008, **5**(6), 373.

31 V. Côté, G. Kos, R. Mortazavi and P. A. Ariya, Microbial and "de novo" transformation of dicarboxylic acids by three airborne fungi, *Sci. Total Environ.*, 2008, **390**(2), 530–537.

32 B. Pastorino, F. Touret, M. Gilles, X. de Lamballerie and R. N. Charrel, Heat Inactivation of Different Types of SARS-CoV-2 Samples: What Protocols for Biosafety, Molecular Detection and Serological Diagnostics?, *Viruses*, 2020, **12**(7), 735.

33 C. Batéjat, Q. Grassin and J. C. Manuguerra, Heat inactivation of the severe acute respiratory syndrome coronavirus 2, *J. Biosaf. Biosecur.*, 2021, **3**(1), 1–3.
34 G. Kampf, A. Voss and S. Scheithauer, Inactivation of coronaviruses by heat, *J. Hosp. Infect.*, 2020, **105**(2), 348–349.
35 E. I. Patterson, T. Prince, E. R. Anderson, A. Casas-Sanchez, S. L. Smith, C. Cansado-Utrilla, *et al.*, Methods of Inactivation of SARS-CoV-2 for Downstream Biological Assays, *J. Infect. Dis.*, 2020, **222**(9), 1462–1467.
36 *SasView*, software. (5.0.4), [cited 2024], available from: **https://www.sasview.org/download/**.
37 S. Bose, D. Pal and P. A. Ariya, On the Role of Starchy Grains in Ice Nucleation Processes, *ACS Food Sci. Technol.*, 2024, **4**(5), 1039–1051.
38 M. Hibbs, *Replication Data for: Physicochemical Properties and Their Impact on Ice Nucleation Efficiency of Respiratory Viral RNA and Proteins*, Borealis, 2024.
39 T. Raatikainen, M. Prank, J. Ahola, H. Kokkola, J. Tonttila and S. Romakkaniemi, The effect of marine ice-nucleating particles on mixed-phase clouds, *Atmos. Chem. Phys.*, 2022, **22**(6), 3763–3778.
40 H. R. Pruppacher and J. D. Klett, *Microphysics of Clouds and Precipitation*, Springer, 2nd edn, 1997.
41 R. L. Hodinka, Respiratory RNA Viruses, *Microbiol. Spectr.*, 2016, **4**(4), 10–128.
42 A. Colas de la Noue, M. Estienney, S. Aho, J.-M. Perrier-Cornet, A. de Rougemont, P. Pothier, *et al.*, Absolute Humidity Influences the Seasonal Persistence and Infectivity of Human Norovirus, *Appl. Environ. Microbiol.*, 2014, **80**(23), 7196–7205.
43 S. Durmuş and K. Ö. Ülgen, Comparative interactomics for virus–human protein–protein interactions: DNA viruses versus RNA viruses, *FEBS Open Bio*, 2017, **7**(1), 96–107.
44 T. Li, A. J. Senesi and B. Lee, Small Angle X-ray Scattering for Nanoparticle Research, *Chem. Rev.*, 2016, **116**(18), 11128–11180.
45 L. Boldon, F. Laliberte and L. Liu, Review of the fundamental theories behind small angle X-ray scattering, molecular dynamics simulations, and relevant integrated application, *Nano Rev.*, 2015, **6**, 25661.
46 R. Wagner, A. Kiselev, O. Möhler, H. Saathoff and I. Steinke, Pre-activation of ice-nucleating particles by the pore condensation and freezing mechanism, *Atmos. Chem. Phys.*, 2016, **16**(4), 2025–2042.
47 M. Fasolo and P. Sollich, Equilibrium Phase Behavior of Polydisperse Hard Spheres, *Phys. Rev. Lett.*, 2003, **91**(6), 068301.
48 S. Auer and D. Frenkel, Quantitative Prediction of Crystal-Nucleation Rates for Spherical Colloids: A Computational Approach, *Annu. Rev. Phys. Chem.*, 2004, **55**(1), 333–361.
49 S. Bose, D. Pal and P. A. Ariya, On the Role of Starchy Grains in Ice Nucleation Processes, *ACS Food Sci. Technol.*, 2024, **4**(5), 1039–1051.
50 L. A. Lee, C. L. Reddington and K. S. Carslaw, On the relationship between aerosol model uncertainty and radiative forcing uncertainty, *Proc. Natl. Acad. Sci. U. S. A.*, 2016, **113**(21), 5820–5827.
51 R. Tignat-Perrier, A. Dommergue, T. M. Vogel and C. Larose, Microbial Ecology of the Planetary Boundary Layer, *Atmosphere*, 2020, **11**(12), 1296.
52 R. Tignat-Perrier, A. Dommergue, A. Thollot, O. Magand, T. M. Vogel and C. Larose, Microbial functional signature in the atmospheric boundary layer, *Biogeosciences*, 2020, **17**(23), 6081–6095.
53 P. Amato, M. Joly, L. Besaury, A. Oudart, N. Taib, A. I. Moné, *et al.*, Active microorganisms thrive among extremely diverse communities in cloud water, *PLoS One*, 2017, **12**(8), e0182869.
54 A. Khaled, M. Zhang, P. Amato, A.-M. Delort and B. Ervens, Biodegradation by bacteria in clouds: an underestimated sink for some organics in the atmospheric multiphase system, *Atmos. Chem. Phys.*, 2021, **21**(4), 3123–3141.
55 P. Amato, L. Besaury, M. Joly, B. Penaud, L. Deguillaume and A.-M. Delort, Metatranscriptomic exploration of microbial functioning in clouds, *Sci. Rep.*, 2019, **9**(1), 4383.
56 H. Li, F. Y. Leong, G. Xu, C. W. Kang, K. H. Lim, B. H. Tan, *et al.*, Airborne dispersion of droplets during coughing: a physical model of viral transmission, *Sci. Rep.*, 2021, **11**(1), 4617.
57 R. Mittal, C. Meneveau and W. Wu, A mathematical framework for estimating risk of airborne transmission of COVID-19 with application to face mask use and social distancing, *Phys. Fluids*, 2020, **32**(10), 101903.
58 K. Lin and L. C. Marr, Humidity-Dependent Decay of Viruses, but Not Bacteria, in Aerosols and Droplets Follows Disinfection Kinetics, *Environ. Sci. Technol.*, 2020, **54**(2), 1024–1032.
59 S. Ratnesar-Shumate, G. Williams, B. Green, M. Krause, B. Holland, S. Wood, *et al.*, Simulated Sunlight Rapidly Inactivates SARS-CoV-2 on Surfaces, *J. Infect. Dis.*, 2020, **222**(2), 214–222.
60 M. Schuit, S. Ratnesar-Shumate, J. Yolitz, G. Williams, W. Weaver, B. Green, *et al.*, Airborne SARS-CoV-2 Is Rapidly Inactivated by Simulated Sunlight, *J. Infect. Dis.*, 2020, **222**(4), 564–571.
61 M. Drexler, *What You Need to Know about Infectious Disease: How Infection Works*, National Academies Press, 2010.
62 N. Mahowald, S. Albani, J. F. Kok, S. Engelstaeder, R. Scanza, D. S. Ward and M. G. Flanner, The size distribution of desert dust aerosols and its impact on the Earth system, *Aeolian Res.*, 2014, **15**, 53–71.
63 K. Tang, B. Sánchez-Parra, P. Yordanova, J. Wehking, A. T. Backes, D. A. Pickersgill, *et al.*, Bioaerosols and atmospheric ice nuclei in a Mediterranean dryland: community changes related to rainfall, *Biogeosciences*, 2022, **19**(1), 71–91.
64 C. Hoose, J. E. Kristjánsson and S. M. Burrows, How important is biological ice nucleation in clouds on a global scale?, *Environ. Res. Lett.*, 2010, **5**(2), 024009.